First Demonstration of Silicon-Based Parallel-Fed Travelling-Wave Photodetector Array (TWPDA)

Xianshu Luo*, Junfeng Song, Qing Fang, Xiaoguang Tu, Lianxi Jia, Tsung-Yang Liow, Mingbin Yu, Guo-Qiang Lo

*Institute of Microelectronics, A*STAR (Agency for Science, Technology and Research), 11 Science Park Road, Singapore Science Park II, Singapore 117685*

**luox@ime.a-star.edu.sg*

Abstract: We demonstrate the first silicon-based parallel-fed travelling-wave photodetector array (TWPDA). Impedance-matched travelling-wave electrode is designed considering periodic loading effect. The demonstrated up to 4-channel TWPDAs show >10GHz 3-dB bandwidths and ~0.75A/W responsivity using 30μm-length PDs.

OCIS codes: (230.0230) Optical devices; (250.0250) Optoelectronics; (040.5160) Photodetectors; (040.6040) Silicon.

1. Introduction

Ge-on-Si photodetector is a key building block for the applications of silicon photonic based optical interconnect and microwave photonics [1]. A photodetector with high power handling capability and high operation speed is particularly important for analog optical link with high gain, low noise floor, and high spurious-free dynamic range [2]. However, there is a trade-off between the photodetector operation bandwidth and the saturation power for the conventional photodetector. In general, the conventional high-speed photodetector is usually designed with low capacitance and small carrier transit time, thus with small absorption volume and consequently cannot achieve high saturation power due to the space charge effect.

In this report, we demonstrate, for the first time to our best knowledge, silicon-based parallel-fed travelling-wave photodetector arrays (TWPDAs) [3-4] with multiple integrated Ge photodetectors, featuring the merits of large operation bandwidth as well as high optical power handling capability. We design the impedance-matched travelling-wave electrode with considering the periodic loading effect induced from the individual Ge photodetector. Dual-layered metal structure is adopted in order for easy design and layout for the impedance-matched travelling-wave electrode. Furthermore, optical delay lines are adopted in each optical channel in order to balance the electrical phase delay. We fabricate such TWPDAs using CMOS-compatible fabrication process in 8 inch SOI wafer with integrating up to four photodetectors. The measured 3-dB bandwidths for 2-channel and 4-channel TWPDA are ~ 14GHz and 12 GHz, respectively, with responsivity of ~ 0.75 A/W.

2. Device Design, Fabrication, and Characterization

Figure 1 shows the block design of the parallel-fed TWPDA. The input light is first split into multiple parallel channels, e.g. *N* channels here, by using low-loss power splitter, such as Y-splitter, or multimode interferometer (MMI) splitter. The light in each of the channel is separately detected by individual high-speed photodetector. The photocurrent is then collected by using large bandwidth impedance-matched travelling-wave electrode in order to maintain the high-speed operation. Furthermore, the optical delay lines are adopted in each optical channel in order to balance the electrical phase delay.

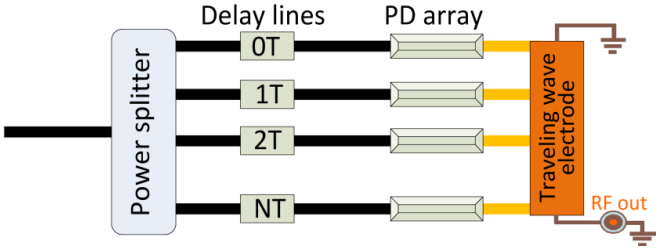

Fig. 1 The block diagram of the parallel-fed travelling-wave photodetector array.

Figure 2 shows the design layout of a 4-channel parallel-fed travelling-wave photodetector array (4-TWPDA). We adopt multi-stage 1×2 MMI splitter for the light splitting, which is modified from our previous design with extremely low loss [5]. We adopt high-speed Ge photodetectors for the light detection [6]. In order for easy design and layout of the impedance-matched travelling-wave electrode, we adopt dual-metal layers, as shown in the zoom-in view of Fig. 2. The first metal layer is the connection to individual Ge photodetector, while the top metal layer is

the impedance-match travelling-wave electrode. We design the impedance-matched travelling-wave electrode with considering the periodic photodetector loading effect [7]. For a symmetric GSG travelling-wave electrode design with 6 μm signal metal width and 4 μm gap separations, the calculated electrical phase velocity is ~ 7.5×10^7 m/s. The Ge photodetector is designed with 5 μm × 30 μm, and the periodicity is 25 μm. For all the travelling-wave electrode design, the ground metal widths are 100 μm. Thus, based on the calculated electrical phase velocity, we design the waveguide-based optical delay lines with unit delay of 0.3 ps, which corresponds to the waveguide length of ~ 25 μm, assuming the group index of ~ 4 for the silicon waveguide.

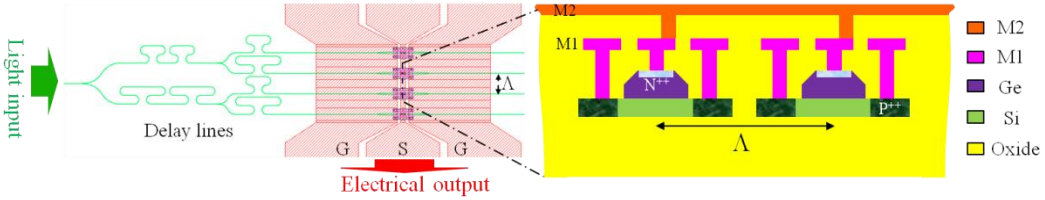

Fig. 2 Design layout of a 4-TWPDA, including the multi-stage MMI-splitter for light splitting, the optical waveguide delay lines, the Ge photodetectors with dual-metal-layered, and the impedance-matched travelling-wave electrode. The zoom-in cross-sectional view shows the dual-metal layers design.

We fabricate the TWPDAs in silicon-on-insulator (SOI) platform by using CMOS-compatible fabrication process. The SOI wafer has a 220nm silicon layer sitting on a 2μm buried oxide (BOX) layer. The device is patterned by using deep ultra-violet (DUV) photolithography, followed by a silicon reactive ion etching (RIE) to form channel waveguides. For the Ge photodetector, separate masks are used for boron implantation to form the P and P^+ Ohmic contacts. The implants are activated using rapid thermal anneal at 1050 °C for 5 seconds. After depositing a thin layer of field oxide, Ge epitaxial windows are opened by a combination of dry and wet etching to expose the underlying Si. After growing a thin SiGe buffer layer at 350 °C, Ge is selectively grown in an ultrahigh vacuum chemical vapor deposition (UHVCVD) epitaxy reactor at 550 °C with a thickness of 500 nm. The N^+ Ohmic contact is formed by implanting phosphorus into Ge top surface, followed by annealing at 500 °C for 5 min. A 0.6 μm-thick oxide insulating layer is deposited, followed by the first contact holes opening, and the deposition and patterning of the first Al metal layer. After another 1.5 μm insulating oxide deposition, the second contact holes to the first metal layer are opened by dry etching process, followed by second Al metal deposition and patterning for the travelling-wave electrode. Finally, more than 100 μm Si trench is etched in order for the light coupling between the lessened optical fiber and the inverse taper waveguide.

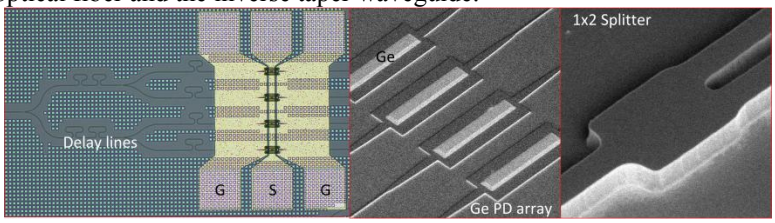

Fig. 3 (a) Optical microscope of the fabricated 4-TWPDA. (b) The SEM of the Ge photodetector array right after the Ge growth. (c) The SEM of the fabricated MMI splitter.

Figure 3(a) shows the optical microscope of a 4-TWPDA based on the design described previously. We design and fabricate 1-, 2-, and 4-TWPDAs in the same silicon chip with the identical designs. The waveguide width is 500 nm and the Ge PD is designed with dimension of 5 μm in width and 30 μm in length. The Ge PD periodicity is designed to be 25 μm, with the optical delay line difference between adjacent channels of 25 μm, in order for velocity matching between optical and electrical signals. Figure 3(b) shows the SEM of the Ge photodetector array before the insulating oxide cladding and metallization, while Fig. 3(c) shows the SEM of the low-loss 1×2 MMI splitter.

We first characterize the optical performance of the basic elements, including the waveguide propagation loss, the MMI splitter insertion loss, etc., in order for the Ge PD responsivity estimation. By using the waveguide cutback structures, we obtained the waveguide propagation loss of -1.5 dB/cm, and the fiber-to-waveguide coupling loss of ~ 2 dB/facet. By using the multi-staged 1×2 MMI splitter structures, we obtained the splitter excess loss of -0.15 dB/channel, which is consistent with our previous demonstration [6].

We then characterize the electrical performance of the TWPDAs by measuring the current-voltage response. Figure 4(a) shows the measurement results with and without light input for 1-, 2-, and 4-TWPDAs. The dark current at -1 V bias is ~ 3 μA for all three types of TWPDAs. In contrast, with a laser output of 5 dBm at 1550 nm, the photocurrent at -1 V bias increases to ~ 0.55 mA. We mention that the optical insertion loss, including the system

loss, the coupling loss, and the waveguide propagation loss, is ~ -6.8 dB before the light is absorbed by the photodetector. With varied input light intensity, we extract the responsivity of ~ 0.75 A/W.

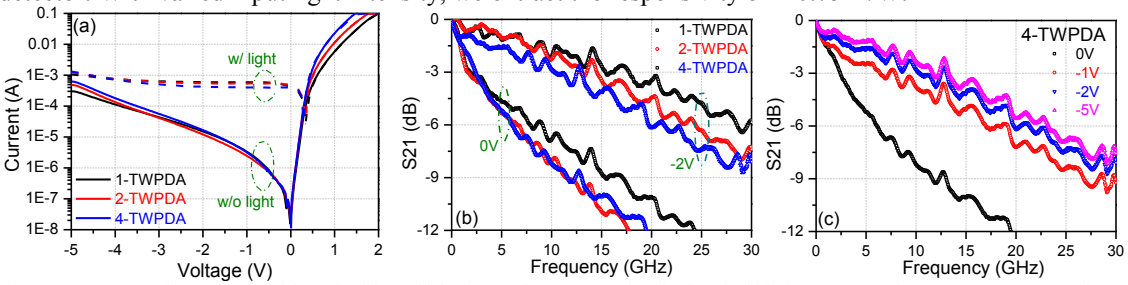

Fig. 4 (a) Measured IV curves with and without light input. (b) Measured 3-dB bandwidth for 1-, 2-, and 4-TWPDA at 0V and -2V bias. (c) Measured 3-dB bandwidth for 4-TWPDA at different biased voltages.

We also measured the opto-electrical response of such TWPDAs by measuring the S21 parameter using a vector network analyzer (VNA). Figure 4(b) shows the normalized S21for 1-, 2-, and 4-TWPDA upon 0V and -2V bias voltages. The 3-dB bandwidths at 0V are ~ 2.5 GHz. Upon -2V bias, the 3-dB bandwidth for 1-TWPDA is ~16 GHz, while decreasing to ~14 GHz and ~12 GHz for 2-, and 4-TWPDAs. We attribute such decrease of the 3-dB bandwidth with the photodetector number increase to the increased lumped capacity arising from the parallel design. In addition, Fig. 4(c) shows the normalized S21 for 4-TWPDA upon different voltage supplies. As the increase of the reverse biased voltages, the 3-dB bandwidth increases. The 3-dB bandwidth at -5V biased voltage is 13 GHz. However, the dark current at -5 V is as high as 0.5 mA, which is not suitable for practical application.

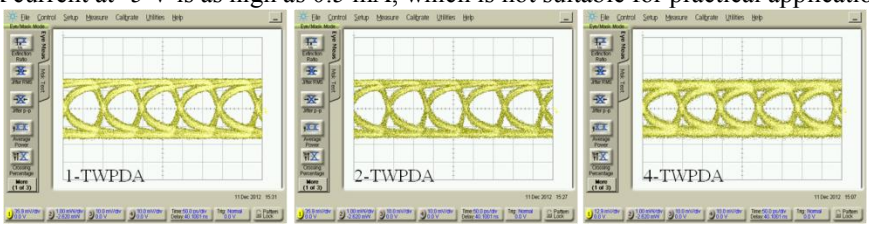

Fig. 5 The measured eye diagrams from the 1-, 2-, and 4-TWPDAs with 10 Gbit/s date rate.

To investigate the signal transmission, we send 10-Gbit/s PRBS signal (bit length 2^{31}-1) to the system and measure the transmitted signal from TWPDAs. The carrier wavelength is selected at 1550 nm. The supplied voltages to the TWPDAs are -2V. Fig. 5 shows the measured eye diagrams from 1-, 2-, and 4-TWPDAs. The open eye diagrams indicate the high-quality data transmission and detection.

3. Summary

We have demonstrated, for the first time to our best knowledge, silicon-based travelling-wave photodetector array (TWPDA) with parallel optical feeding. The impedance-matched travelling-wave electrode is designed the Ge PD loading effect in mind. Optical delay lines are designed to balance the electrical phase delay. We demonstrated up to 4-channel TWPDA with 3-dB bandwidth of ~12 GHz and responsivity of ~ 0.75 A/W. The power handling capability of such TWPDAs is under characterization. Such traveling-wave electrode photodetector array has wide applications such as optical communication, optical interconnection, and microwave photonics.

This work was supported by the Science and Engineering Research Council of A*STAR (Agency for Science, Technology and Research), Singapore, under SERC grant number: 122 331 0076.

4. References

[1]. J. Michel, J. Liu, and L.C. Kimerling, "High-performance Ge-on-Si photodetectors," Nat. Photonics **4**, 527-534 (2010).
[2]. V. M. Hietala, G. A. Vawter, T. M. Brennan, and B. E. Hammons, "Travelling-wave photodetectors for high-power, large-bandwidth applications," IEEE Trans. Microw. Theory Tech. **43**, 2291-2298 (1995).
[3]. K. S. Giboney, M. J. W. Rodwell, and J. E. Bowers, "Traveling-wave photodetector theory," IEEE Trans. Microw. Theory Tech. **45**, 1310-1319 (1997).
[4]. Andreas Beling, Joe C. Campbell, Heinz-Gunter Bach, Gebre Giorgis Mekonnen, and Detlef Schmidt, "Parallel-eed traveling wave photodetector for >100-GHz applications," J. Lightwave Technol. **26**, 16-20 (2008).
[5]. Z. Xiao, X. Luo, P. H. Lim, P. Prabhathan, S. T. H. Silalahi, T.-Y. Liow, J. Zhang, and F. Luan, "Ultra-compact low loss polarization insensitive silicon waveguide splitter," Opt. Express **21**, 16331-16336 (2013).
[6]. T. Y. Liow, K. W. Ang, Q. Fang, J. Song, Y. Xiong, M. Yu, G. Q. Lo, and D. L. Kwong, "Silicon modulators and germanium photodetectors on SOI: monolithic integration, compatibility, and performance optimization," IEEE J. Sel. Top. Quantum Electron. **16**, 307-315 (2010).
[7]. L. Y. Lin, M. C. Wu, T. Itoh, T. A. Vang, R. E. Muller, D. L. Sivco, and A. Y. Cho, "High-power high-speed photodetectors-design, analysis, and experimental demonstration," IEEE Trans. Microw. Theory Tech. **45**, 1320-1331 (1997).